Four-fermion production in e^+e^- collisions at centre-of-mass energies of 130 and 136 GeV

D. Buskulic, I. de Bonis, D. Decamp, P. Ghez, C. Goy, J.P. Lees, A. Lucotte, M.N. Minard, J.Y. Nief, P. Odier, et al.

CERN-PPE/96-088
27 June 1996

Four-fermion production in e^+e^- collisions at centre-of-mass energies of 130 and 136 GeV

The ALEPH Collaboration

Abstract

Four-fermion events have been selected in a data sample of 5.8 pb^{-1} collected with the ALEPH detector at centre-of-mass energies of 130 and 136 GeV. The final states $\ell^+\ell^- q\bar{q}$, $\ell^+\ell^-\ell^+\ell^-$, $\nu\bar{\nu}q\bar{q}$, and $\nu\bar{\nu}\ell^+\ell^-$ have been examined. Five events are observed in the data, in agreement with the Standard Model predictions of 6.67 ± 0.38 events from four-fermion processes and $0.14 \pm^{0.19}_{0.05}$ from background processes.

(Submitted to Physics Letters B)

See following pages for the list of authors

The ALEPH Collaboration

D. Buskulic, I. De Bonis, D. Decamp, P. Ghez, C. Goy, J.-P. Lees, A. Lucotte, M.-N. Minard, J.-Y. Nief, P. Odier, B. Pietrzyk

Laboratoire de Physique des Particules (LAPP), IN^{2}P^3-CNRS, 74019 Annecy-le-Vieux Cedex, France

M.P. Casado, M. Chmeissani, J.M. Crespo, M. Delfino, I. Efthymiopoulos,[20] E. Fernandez, M. Fernandez-Bosman, Ll. Garrido,[15] A. Juste, M. Martinez, S. Orteu, C. Padilla, I.C. Park, A. Pascual, J.A. Perlas, I. Riu, F. Sanchez, F. Teubert

Institut de Fisica d'Altes Energies, Universitat Autonoma de Barcelona, 08193 Bellaterra (Barcelona), Spain[7]

A. Colaleo, D. Creanza, M. de Palma, G. Gelao, M. Girone, G. Iaselli, G. Maggi,[3] M. Maggi, N. Marinelli, S. Nuzzo, A. Ranieri, G. Raso, F. Ruggieri, G. Selvaggi, L. Silvestris, P. Tempesta, G. Zito

Dipartimento di Fisica, INFN Sezione di Bari, 70126 Bari, Italy

X. Huang, J. Lin, Q. Ouyang, T. Wang, Y. Xie, R. Xu, S. Xue, J. Zhang, L. Zhang, W. Zhao

Institute of High-Energy Physics, Academia Sinica, Beijing, The People's Republic of China[8]

R. Alemany, A.O. Bazarko, M. Cattaneo, P. Comas, P. Coyle, H. Drevermann, R.W. Forty, M. Frank, R. Hagelberg, J. Harvey, P. Janot, B. Jost, E. Kneringer, J. Knobloch, I. Lehraus, G. Lutters, E.B. Martin, P. Mato, A. Minten, R. Miquel, Ll.M. Mir,[2] L. Moneta, T. Oest,[1] A. Pacheco, J.-F. Pusztaszeri, F. Ranjard, P. Rensing,[25] L. Rolandi, D. Schlatter, M. Schmelling,[24] M. Schmitt, O. Schneider, W. Tejessy, I.R. Tomalin, A. Venturi, H. Wachsmuth, A. Wagner

European Laboratory for Particle Physics (CERN), 1211 Geneva 23, Switzerland

Z. Ajaltouni, A. Barrès, C. Boyer, A. Falvard, P. Gay, C . Guicheney, P. Henrard, J. Jousset, B. Michel, S. Monteil, J-C. Montret, D. Pallin, P. Perret, F. Podlyski, J. Proriol, P. Rosnet, J.-M. Rossignol

Laboratoire de Physique Corpusculaire, Université Blaise Pascal, IN^{2}P^3-CNRS, Clermont-Ferrand, 63177 Aubière, France

T. Fearnley, J.B. Hansen, J.D. Hansen, J.R. Hansen, P.H. Hansen, B.S. Nilsson, B. Rensch, A. Wäänänen

Niels Bohr Institute, 2100 Copenhagen, Denmark[9]

A. Kyriakis, C. Markou, E. Simopoulou, A. Vayaki, K. Zachariadou

Nuclear Research Center Demokritos (NRCD), Athens, Greece

A. Blondel, J.C. Brient, A. Rougé, M. Rumpf, A. Valassi,[6] H. Videau[21]

Laboratoire de Physique Nucléaire et des Hautes Energies, Ecole Polytechnique, IN^{2}P^3-CNRS, 91128 Palaiseau Cedex, France

E. Focardi,[21] G. Parrini

Dipartimento di Fisica, Università di Firenze, INFN Sezione di Firenze, 50125 Firenze, Italy

M. Corden, C. Georgiopoulos, D.E. Jaffe

Supercomputer Computations Research Institute, Florida State University, Tallahassee, FL 32306-4052, USA[13,14]

A. Antonelli, G. Bencivenni, G. Bologna,[4] F. Bossi, P. Campana, G. Capon, D. Casper, V. Chiarella, G. Felici, P. Laurelli, G. Mannocchi,[5] F. Murtas, G.P. Murtas, L. Passalacqua, M. Pepe-Altarelli

Laboratori Nazionali dell'INFN (LNF-INFN), 00044 Frascati, Italy

L. Curtis, S.J. Dorris, A.W. Halley, I.G. Knowles, J.G. Lynch, V. O'Shea, C. Raine, P. Reeves, J.M. Scarr, K. Smith, P. Teixeira-Dias, A.S. Thompson, F. Thomson, S. Thorn, R.M. Turnbull

Department of Physics and Astronomy, University of Glasgow, Glasgow G12 8QQ,United Kingdom[10]

U. Becker, C. Geweniger, G. Graefe, P. Hanke, G. Hansper, V. Hepp, E.E. Kluge, A. Putzer, M. Schmidt, J. Sommer, H. Stenzel, K. Tittel, S. Werner, M. Wunsch

Institut für Hochenergiephysik, Universität Heidelberg, 69120 Heidelberg, Fed. Rep. of Germany[16]

D. Abbaneo, R. Beuselinck, D.M. Binnie, W. Cameron, P.J. Dornan, P. Morawitz, A. Moutoussi, J. Nash, J.K. Sedgbeer, A.M. Stacey, M.D. Williams

Department of Physics, Imperial College, London SW7 2BZ, United Kingdom[10]

G. Dissertori, P. Girtler, D. Kuhn, G. Rudolph

Institut für Experimentalphysik, Universität Innsbruck, 6020 Innsbruck, Austria[18]

A.P. Betteridge, C.K. Bowdery, P. Colrain, G. Crawford, A.J. Finch, F. Foster, G. Hughes, T. Sloan, E.P. Whelan, M.I. Williams

Department of Physics, University of Lancaster, Lancaster LA1 4YB, United Kingdom[10]

A. Galla, A.M. Greene, C. Hoffmann, K. Jacobs, K. Kleinknecht, G. Quast, B. Renk, E. Rohne, H.-G. Sander, P. van Gemmeren C. Zeitnitz

Institut für Physik, Universität Mainz, 55099 Mainz, Fed. Rep. of Germany[16]

J.J. Aubert,[21] A.M. Bencheikh, C. Benchouk, A. Bonissent, G. Bujosa, D. Calvet, J. Carr, C. Diaconu, N. Konstantinidis, P. Payre, D. Rousseau, M. Talby, A. Sadouki, M. Thulasidas, A. Tilquin, K. Trabelsi

Centre de Physique des Particules, Faculté des Sciences de Luminy, IN^{2}P^3-CNRS, 13288 Marseille, France

M. Aleppo, F. Ragusa[21]

Dipartimento di Fisica, Universitá di Milano e INFN Sezione di Milano, 20133 Milano, Italy.

C. Bauer, R. Berlich, W. Blum, V. Büscher, H. Dietl, F. Dydak,[21] G. Ganis, C. Gotzhein, H. Kroha, G. Lütjens, G. Lutz, W. Männer, H.-G. Moser, R. Richter, A. Rosado-Schlosser, S. Schael, R. Settles, H. Seywerd, R. St. Denis, H. Stenzel, W. Wiedenmann, G. Wolf

Max-Planck-Institut für Physik, Werner-Heisenberg-Institut, 80805 München, Fed. Rep. of Germany[16]

J. Boucrot, O. Callot, A. Cordier, M. Davier, L. Duflot, J.-F. Grivaz, Ph. Heusse, A. Höcker, A. Jacholkowska, M. Jacquet, D.W. Kim,[19] F. Le Diberder, J. Lefrançois, A.-M. Lutz, I. Nikolic, H.J. Park,[19] M.-H. Schune, S. Simion, J.-J. Veillet, I. Videau, D. Zerwas

Laboratoire de l'Accélérateur Linéaire, Université de Paris-Sud, IN^{2}P^3-CNRS, 91405 Orsay Cedex, France

P. Azzurri, G. Bagliesi, G. Batignani, S. Bettarini, C. Bozzi, G. Calderini, M. Carpinelli, M.A. Ciocci, V. Ciulli, R. Dell'Orso, R. Fantechi, I. Ferrante, A. Giassi, A. Gregorio, F. Ligabue, A. Lusiani, P.S. Marrocchesi, A. Messineo, F. Palla, G. Rizzo, G. Sanguinetti, A. Sciabà, P. Spagnolo, J. Steinberger, R. Tenchini, G. Tonelli,[26] C. Vannini, P.G. Verdini, J. Walsh

Dipartimento di Fisica dell'Università, INFN Sezione di Pisa, e Scuola Normale Superiore, 56010 Pisa, Italy

G.A. Blair, L.M. Bryant, F. Cerutti, J.T. Chambers, Y. Gao, M.G. Green, T. Medcalf, P. Perrodo, J.A. Strong, J.H. von Wimmersperg-Toeller

Department of Physics, Royal Holloway & Bedford New College, University of London, Surrey TW20 OEX, United Kingdom[10]

D.R. Botterill, R.W. Clifft, T.R. Edgecock, S. Haywood, P. Maley, P.R. Norton, J.C. Thompson, A.E. Wright

Particle Physics Dept., Rutherford Appleton Laboratory, Chilton, Didcot, Oxon OX11 OQX, United Kingdom[10]

B. Bloch-Devaux, P. Colas, S. Emery, W. Kozanecki, E. Lançon, M.C. Lemaire, E. Locci, B. Marx, P. Perez, J. Rander, J.-F. Renardy, A. Roussarie, J.-P. Schuller, J. Schwindling, A. Trabelsi, B. Vallage

CEA, DAPNIA/Service de Physique des Particules, CE-Saclay, 91191 Gif-sur-Yvette Cedex, France[17]

S.N. Black, J.H. Dann, R.P. Johnson, H.Y. Kim, A.M. Litke, M.A. McNeil, G. Taylor

Institute for Particle Physics, University of California at Santa Cruz, Santa Cruz, CA 95064, USA[22]

C.N. Booth, R. Boswell, C.A.J. Brew, S. Cartwright, F. Combley, A. Koksal, M. Letho, W.M. Newton, J. Reeve, L.F. Thompson

Department of Physics, University of Sheffield, Sheffield S3 7RH, United Kingdom[10]

A. Böhrer, S. Brandt, G. Cowan, C. Grupen, P. Saraiva, L. Smolik, F. Stephan,

Fachbereich Physik, Universität Siegen, 57068 Siegen, Fed. Rep. of Germany[16]

M. Apollonio, L. Bosisio, R. Della Marina, G. Giannini, B. Gobbo, G. Musolino

Dipartimento di Fisica, Università di Trieste e INFN Sezione di Trieste, 34127 Trieste, Italy

Experimental Elementary Particle Physics, University of Washington, WA 98195 Seattle, U.S.A.

S.R. Armstrong, P. Elmer, Z. Feng,[12] D.P.S. Ferguson, Y.S. Gao,[23] S. González, J. Grahl, T.C. Greening, O.J. Hayes, H. Hu, P.A. McNamara III, J.M. Nachtman, W. Orejudos, Y.B. Pan, Y. Saadi, I.J. Scott, A.M. Walsh,[27] Sau Lan Wu, X. Wu, J.M. Yamartino, M. Zheng, G. Zobernig

Department of Physics, University of Wisconsin, Madison, WI 53706, USA[11]

[1] Now at DESY, Hamburg, Germany.
[2] Supported by Dirección General de Investigación Científica y Técnica, Spain.
[3] Now at Dipartimento di Fisica, Università di Lecce, 73100 Lecce, Italy.
[4] Also Istituto di Fisica Generale, Università di Torino, Torino, Italy.
[5] Also Istituto di Cosmo-Geofisica del C.N.R., Torino, Italy.
[6] Supported by the Commission of the European Communities, contract ERBCHBICT941234.
[7] Supported by CICYT, Spain.
[8] Supported by the National Science Foundation of China.
[9] Supported by the Danish Natural Science Research Council.
[10] Supported by the UK Particle Physics and Astronomy Research Council.
[11] Supported by the US Department of Energy, grant DE-FG0295-ER40896.
[12] Now at The Johns Hopkins University, Baltimore, MD 21218, U.S.A.
[13] Supported by the US Department of Energy, contract DE-FG05-92ER40742.
[14] Supported by the US Department of Energy, contract DE-FC05-85ER250000.
[15] Permanent address: Universitat de Barcelona, 08208 Barcelona, Spain.
[16] Supported by the Bundesministerium für Forschung und Technologie, Fed. Rep. of Germany.
[17] Supported by the Direction des Sciences de la Matière, C.E.A.
[18] Supported by Fonds zur Förderung der wissenschaftlichen Forschung, Austria.
[19] Permanent address: Kangnung National University, Kangnung, Korea.
[20] Now at CERN, 1211 Geneva 23, Switzerland.
[21] Also at CERN, 1211 Geneva 23, Switzerland.
[22] Supported by the US Department of Energy, grant DE-FG03-92ER40689.
[23] Now at Harvard University, Cambridge, MA 02138, U.S.A.
[24] Now at Max-Plank-Institüt für Kernphysik, Heidelberg, Germany.
[25] Now at Dragon Systems, Newton, MA 02160, U.S.A.
[26] Also at Istituto di Matematica e Fisica, Università di Sassari, Sassari, Italy.
[27] Now at Rutgers University, Piscataway, NJ 08855-0849, U.S.A.

1 Introduction

An understanding of four-fermion processes is essential in the search for new particles at LEP. These processes have signatures which could mimic signals from new physics such as missing energy (SUSY production, H$\nu\bar{\nu}$ final state) or energetic lepton pairs (H$\ell^+\ell^-$ final states). Given the relatively clean signature of four-fermion events, a deviation from the Standard Model expectations could be an indication of new physics.

Studies of four-fermion processes have been performed at LEP 1 [1, 2] and at lower centre-of-mass energies [3]. The recent increase in the LEP centre-of-mass energy from the Z peak to 130 and 136 GeV allows the probing of higher Q^2 in the four-fermion process.

Four-fermion events involving only γ or Z exchange are produced within the Standard Model in processes with the diagrams shown in Fig. 1. At these energies, as well as at LEP 1, the four-fermion production cross section is dominated by neutral gauge boson exchange. However, the relative contributions from the various diagrams are different from those of LEP 1. The contribution from diagrams with W's is negligible.

The final states considered in this analysis can be classified as follows:

- two charged leptons and two quarks ($\ell^+\ell^-\mathrm{q\bar{q}}$);
- four charged leptons ($\ell^+\ell^-\ell^+\ell^-$ and $\ell^+\ell^-\tau^+\tau^-$);
- two neutrinos and two quarks ($\nu\bar{\nu}\mathrm{q\bar{q}}$);
- two neutrinos and two charged leptons ($\nu\bar{\nu}\ell^+\ell^-$).

Unless otherwise noted, "ℓ" stands for electron or muon. Not considered in this letter are the $\mathrm{q\bar{q}q\bar{q}}$, $\ell\nu\mathrm{q\bar{q}}$, and $\nu\bar{\nu}\nu\bar{\nu}$ final states. The $\mathrm{q\bar{q}q\bar{q}}$ final state is difficult to distinguish from QCD $\mathrm{q\bar{q}}$ production and has been studied elsewhere [4]. The $\ell\nu\mathrm{q\bar{q}}$ final state is only produced by W exchange and thus has a negligible production rate at $\sqrt{s}$ = 130 and 136 GeV.

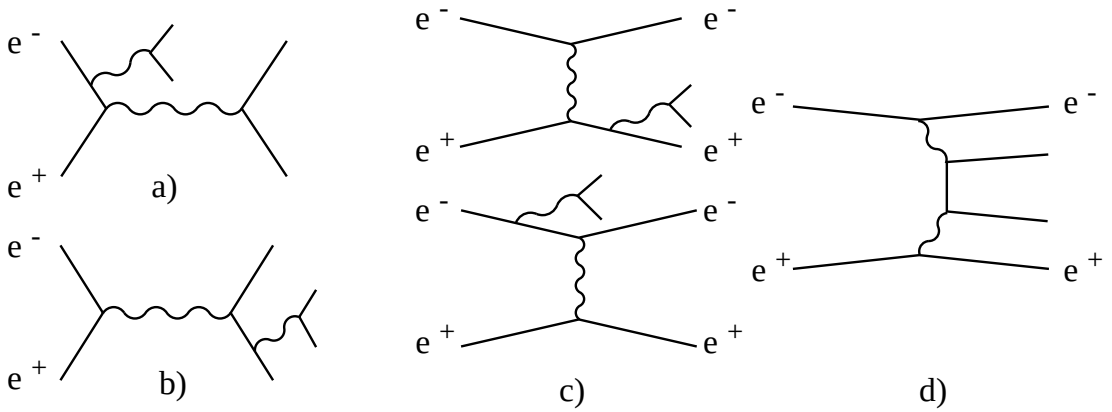

Figure 1: Feynman diagrams for four-fermion final states involving only γ or Z exchange: a) conversion, b) annihilation, c) Bremsstrahlung, d) multiperipheral. The wiggly lines represent a γ or a Z exchange. The solid lines not labelled as $e^{\pm}$ may be quarks or leptons.

This paper is organised as follows. After a brief description of the relevant components of the ALEPH detector, the Monte Carlo and data samples are described. The details of the analyses in the four main channels are then given, including selection requirements and expectations. The results are summarized at the end.

2 The ALEPH Detector

The ALEPH detector is described in detail in Ref. [5]. An account of the performance of the detector and a description of the standard analysis algorithms are found in Ref. [6]. Here, only a brief description of the detector elements and the algorithms relevant to this analysis is given.

In ALEPH, the trajectories of charged particles are measured with a silicon vertex detector (VDET), a cylindrical drift chamber (ITC), and a large time projection chamber (TPC), all immersed in a 1.5 T magnetic field provided by a superconducting solenoidal coil. The energy of electrons, photons, and hadrons is measured with the electromagnetic (ECAL), the hadron (HCAL), and the luminosity calorimeters (LCAL and SICAL). The ECAL, placed between the TPC and the coil, is a highly segmented calorimeter which is used in identifying electrons and photons and in measuring their energy and position. The LCAL and SICAL extend the calorimetric coverage down to 24 mrad from the beam axis. The HCAL consists of an instrumented iron return yoke. It provides a measurement of hadronic energy and, together with external chambers, muon identification.

Global event quantities are measured with an energy flow algorithm. This algorithm combines individual calorimeter and tracker measurements into energy flow "objects". These objects are classified as photons, neutral hadrons, and charged particles, and some are further identified as electrons or muons.

In this analysis, good charged particle tracks are selected by requiring that they be reconstructed with at least four hits in the TPC and that they originate from within a cylinder of length 20 cm and radius 2 cm centered at the nominal interaction point. Track segments which do not fulfill the above requirements are labelled as bad tracks.

This analysis makes use of lepton identification and all channels use the same lepton identification criteria when applicable. In ALEPH, electrons are identified by comparing the momentum measured by the tracking detectors with the energy measured in the ECAL, by the depth and shape of the ECAL shower, and by the specific ionization information from the TPC when available. Muons are identified by their characteristic hit pattern in the hadron calorimeter and if they have at least one associated hit in the muon chambers. Lepton identification in ALEPH is described in detail in Ref. [7].

Converted photons constitute an important background in all channels. A pair of oppositely-charged particle tracks is identified as a converted photon if the pair mass, when computed at the conversion point, is less than 40 MeV/c^2 and the materialization occurs more than 4 cm away from the primary vertex (just inside the VDET). In addition, the distance between the two tracks at the point of closest approach is required to be less than 1 cm in a plane transverse to the beam, and less than 3 cm along the beam axis. In this analysis, conversion electrons are also rejected by requiring that electron tracks have at least one hit in the VDET. This requirement eliminates electrons from photons which materialize outside of the VDET volume.

3 Event Samples

The data used in this analysis correspond to an integrated luminosity of $\mathcal{L} = 5.8$ pb^{-1} collected in November 1995. The luminosity was about equally shared between the two centre-of-mass energies of 130 and 136 GeV.

The four-fermion processes were simulated with the FERMISV [8] Monte Carlo program, which includes all diagrams of Fig. 1, initial and final state radiation, and QCD corrections to the propagator at low Q^2 [1]. (The latter is especially relevant for the study of the low-multiplicity hadronic final states.) Difermion masses were free to be as small as kinematically

allowed. The charged leptons were required to make an angle of at least 10° with respect to the beam axis and to have a minimum momentum of 0.5 GeV/c.

The hadronic ($q\bar{q}$) background Monte Carlo sample used was generated with PYTHIA 5.7 [9]. Dimuon and ditau samples were generated using KORALZ 4.0 [10]. The Bhabha Monte Carlo samples were generated with both the BABAMC [11] and UNIBAB [12] Monte Carlo programs. Preselected samples of gamma-gamma interactions were generated using PHOT02 [13] and GGMJET [14]. Although such events come mainly from the multiperipheral diagram of Fig. 1, most of them have one or two electrons ("singly-tagged" or "untagged" events) escaping undetected along the beam axis and would not fulfill a four-(detected) fermion final state requirement. Thus, untagged and singly-tagged gamma-gamma interactions have been treated as an independent background in this analysis.

All Monte Carlo samples used in this analysis correspond to at least 25 times the equivalent data luminosity.

4 Event Selection

4.1 Event properties

The conversion diagram (Fig. 1a) dominates four-fermion production at $\sqrt{s}$ = 130 and 136 GeV, except for diagrams involving electrons in the final state. This contrasts with the situation at LEP 1, where the dominant contribution comes from the annihilation process. Typically, the conversion diagram consists of an initial state virtual photon recoiling against an on-shell Z boson. At these energies, however, most on-shell Z's are produced in conjunction with a real initial state photon (hereafter called "radiative return to the Z"). In the case of four-fermions, the topology of this boosted Z decay is characterized by one pair of high-mass ($M_{\mathrm{f\bar{f}}} \approx M_{\mathrm{Z}}$) and one pair of low-mass ($M^2_{\mathrm{f\bar{f}}} \approx Q^2$ of photon propagator) fermions. The $\ell^+\ell^-\mathrm{q\bar{q}}$ and $\ell^+\ell^-\ell^+\ell^-$ channels have clear signatures characterized by energetic isolated leptons and no missing energy. Since at these energies neutrino pairs are mostly produced via the Z propagator, the neutrino channels are distinguished by large missing energy and missing masses consistent with M_{Z}. The situation is different for final states with electrons for which the t-channel diagrams (Fig. 1c) have a non-negligible contribution.

Although kinematically similar, the four-fermion final states have distinctive signatures and different background sources. This analysis therefore consists of individual searches for each of the four-fermion final states. In the following, a description of each event selection is presented together with the Standard Model expectation in each topology.

4.2 The $\ell^+\ell^-\mathrm{q\bar{q}}$ channel

This channel is characterized by either a low mass isolated lepton pair recoiling against a high multiplicity hadronic system or a high mass lepton pair and a low multiplicity hadronic system. This analysis was designed to be efficient for both the low- and the high-multiplicity final states.

A sample of hadronic events is preselected by requiring that the event be inconsistent with a radiative return to the Z. In each event, tracks from photon conversions are removed from further consideration. Events are required to have at least four good charged particle tracks. The event visible mass, M_{vis}, and longitudinal momentum, P_z^{vis}, calculated from all energy-flow objects, are required to satisfy $M_{\mathrm{vis}} - |P_z^{\mathrm{vis}}| > 0.5\sqrt{s}$ in order to reject longitudinally imbalanced events. Hadronic events with initial state radiation are further rejected with the

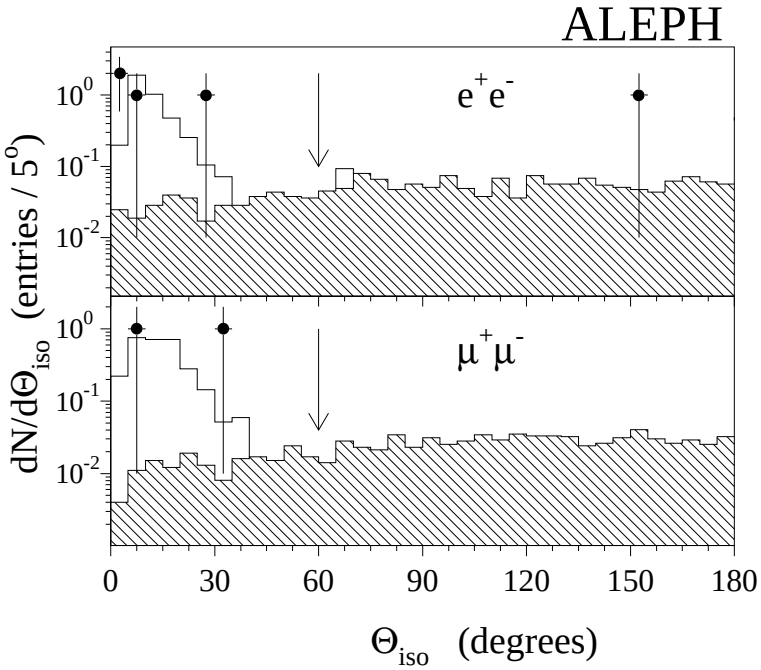

Figure 2: The lepton pair isolation, $\Theta_{\rm iso}$, for $\mathrm{e^+e^-q\bar{q}}$ and $\mu^+\mu^-\mathrm{q\bar{q}}$ candidates after all cuts (except isolation) have been applied. Presented are the expectations from FERMISV (hatched), the background (mostly $\mathrm{q\bar{q}}$, solid) and the data (dots). The histograms are normalized to the expectations in 5.8 pb^{-1} of data. The cut $\Theta_{\rm iso} > 60^\circ$ is indicated with an arrow.

requirement that there be no significant energy depositions in the luminosity calorimeters, *i.e.,* that $E_{\rm LCAL} + E_{\rm SICAL} < 20$ GeV.

Only events with at least two oppositely-charged leptons of the same type with total energy $E_{\ell^+} + E_{\ell^-} > 0.10\sqrt{s}$ are kept. In order to further reject backgrounds in the low-multiplicity events, some additional cuts are imposed. In $\mathrm{e^+e^-q\bar{q}}$ [$\mu^+\mu^-\mathrm{q\bar{q}}$] events with less than seven charged particle tracks, the number of electrons is required to be $N_{\rm e} = 2$ [$N_{\rm e} = 0$], while the number of muons is required to be $N_\mu = 0$ [$N_\mu = 2$]. In addition, the number of tracks with at least one VDET hit must be at least four [three]. Bhabha events with photon conversions which still pass the above cuts are eliminated by requiring that the electrons in an $\mathrm{e^+e^-q\bar{q}}$ event have energies which do not exceed $90\% E_{\rm beam}$ and that each electron has at least one VDET hit.

After the above requirements, one last cut is placed on the lepton pair isolation. The lepton pair isolation is defined as the sum of the individual isolation angles of each lepton, $\Theta_{\rm iso} = \theta^1_{\rm iso} + \theta^2_{\rm iso}$. For each lepton i, the angle $\theta^i_{\rm iso}$ is the half-angle of the largest cone around the lepton momentum direction containing less than 5% of the visible energy of all particles in the event except the two leptons. In order to avoid losses due to Bremsstrahlung, a 1° cone around each lepton is also excluded from the energy sum. For both the $\mathrm{e^+e^-q\bar{q}}$ and $\mu^+\mu^-\mathrm{q\bar{q}}$ cases, a cut of $\Theta_{\rm iso} > 60^\circ$ is imposed. Fig. 2 shows the $\Theta_{\rm iso}$ distribution for data and Monte Carlo, normalized to the integrated luminosity.

The expectations for the $\ell^+\ell^-\mathrm{q\bar{q}}$ channel are summarized in Table 1. The signal expectations

Table 1: Summary of $\ell^+\ell^-q\bar{q}$ expectations. The uncertainties are statistical only.

Process	$q\bar{q}$	$\ell^+\ell^-\gamma$	$\gamma\gamma \to f\bar{f}$	$\ell^+\ell^-\ell^+\ell^-$	$\ell^+\ell^-q\bar{q}$
N expected, $e^+e^-q\bar{q}$	$0.04 \pm^{0.06}_{0.03}$	$0.01 \pm^{0.07}_{0}$	$0.01 \pm^{0.01}_{0}$	0.04 ± 0.01	1.69 ± 0.06
Efficiency					$(16 \pm 1)\%$
N expected, $\mu^+\mu^-q\bar{q}$	< 0.05	< 0.01	< 0.07	0.03 ± 0.00	0.89 ± 0.03
Efficiency					$(36 \pm 1)\%$

include a correction for gluon radiation (discussed in Section 4.5). Although this analysis is not designed to select the $\tau^+\tau^-q\bar{q}$ channel, a total of 0.01 events are expected from the $e^+e^-q\bar{q}$ and $\mu^+\mu^-q\bar{q}$ selections; the $\tau^+\tau^-q\bar{q}$ predictions are included in the $e^+e^-q\bar{q}$ and $\mu^+\mu^-q\bar{q}$ expectations of Table 1. Table 1 also includes an entry for $\ell^+\ell^-\ell^+\ell^-$ signal. These processes are mostly $\tau^+\tau^-e^+e^-$ and $\tau^+\tau^-\mu^+\mu^-$ four-fermion final states in which the tau leptons decay into hadrons and are thus indistinguishable from low-multiplicity $\ell^+\ell^-q\bar{q}$ final states. This cross-efficiency between the $\ell^+\ell^-q\bar{q}$ and the $\ell^+\ell^-\ell^+\ell^-$ channels is included in the total expectations presented in Section 5. The efficiency presented in Table 1 is computed inside the acceptance region defined by FERMISV.

The total number of expected background events is $0.06\,^{+\,0.09}_{-\,0.03}$ for $e^+e^-q\bar{q}$ and $0\,^{+\,0.09}_{-\,0}$ for $\mu^+\mu^-q\bar{q}$, while the expectation from $\ell^+\ell^-q\bar{q}$ four-fermion states, as predicted by FERMISV, is 1.69 ± 0.06 events for $e^+e^-q\bar{q}$ and 0.89 ± 0.03 events for $\mu^+\mu^-q\bar{q}$, where the uncertainties are statistical only. The assignment of systematic uncertainties is discussed in Section 4.5.

4.3 The four-lepton channel

The signature of four charged leptons is very clean, but the cross section for this channel is small, due to the low branching ratio of Z decaying to charged leptons. Since the tau channel is expected to contribute a third of the signal, the analysis includes a selection which is efficient for tau leptons.

The selection relies mainly on the number of good charged particle tracks, a minimum number of identified leptons, and the rejection of converted photons. It is similar for both the $\ell^+\ell^-\ell^+\ell^-$ and $\ell^+\ell^-\tau^+\tau^-$ topologies, so the cuts for the preselection are given for the $\ell^+\ell^-\ell^+\ell^-$ case, with differences for the $\ell^+\ell^-\tau^+\tau^-$ case indicated in square brackets. Events with a visible energy $E_{\rm vis} > 0.6\sqrt{s}$ $[0.2\sqrt{s}]$ and missing mass $M_{\rm miss} < 0.25\sqrt{s}$ $[0.7\sqrt{s}]$ are selected, which rejects gamma-gamma and ditau events. Events are required to have four [or six] good tracks, with a total charge of zero. No [two or less] bad tracks are allowed, reducing backgrounds with nuclear interactions and soft converted photons. The number of identified leptons in the event is required to be $N_e + N_\mu \geq 2$ $[N_e \geq 2$ or $N_\mu \geq 2]$. In addition, at least two of the good tracks must have a minimum P_T with respect to the beam of 2 GeV/c. In events where there are no four identified muons, the two oppositely-charged particle tracks forming the smallest invariant mass are paired, and labelled tracks 1 and 2. Tracks 1 and 2 must not be consistent with a photon conversion, and in addition, they must both have at least one VDET hit if their invariant mass is less than 10 GeV/c^2.

After the above preselection, additional cuts are applied to the $\ell^+\ell^-\ell^+\ell^-$ topology. The sum of the energies of the remaining two tracks (tracks labelled 3 and 4) is required to be greater than 40 GeV, as expected for leptons from Z decays. In order to reject t-channel Bhabha events, the momentum vector difference between tracks 3 and 4 must make an angle of at least 18.2° with respect to the beam axis. Background from real converted Bremsstrahlung photons is eliminated by requiring that the photon candidate formed by tracks 1 and 2 (if $M_{12} < 1$ GeV/c^2) be acollinear with tracks 3 and 4. To this end, if there are fewer than four identified muons or less than three electrons in the event, then the vector momentum sum of tracks 1 and 2 must make an angle of at least 2° with both tracks 3 and 4. If there are three or more electrons in the event, then this last cut is tightened to 5°. Finally, the sum of charged particle energies is required to be $E_{\rm ch} > 0.8E_{\rm vis}$.

For the $\ell^+\ell^-\tau^+\tau^-$ topology, events are required to satisfy $E_{\rm vis} < 0.9\sqrt{s}$, as expected for events with neutrinos, and to contain no converted photons. The JADE algorithm [15] is used to form jets from all objects aside from tracks 1 and 2, with $y_{\rm cut} = (3$ GeV/$c^2)^2/s$, and only

Table 2: The expectations for four-lepton events. The uncertainties are statistical only.

Process
N events expected
Efficiency
$e^+e^-e^+e^-$
0.89 ± 0.06
$(11 \pm 1)\%$
$e^+e^-\mu^+\mu^-$
0.49 ± 0.02
$(31 \pm 2)\%$
$\mu^+\mu^-\mu^+\mu^-$
0.09 ± 0.00
$(72 \pm 1)\%$
$e^+e^-\tau^+\tau^-$
0.09 ± 0.01
$(19 \pm 1)\%$
$\mu^+\mu^-\tau^+\tau^-$
0.04 ± 0.00
$(29 \pm 1)\%$
$\ell^+\ell^-q\bar{q}$
0.32 ± 0.06
BACKGROUND
$0.01\ ^{+\ 0.08}_{-\ 0.01}$

events with two or three well-contained jets ($|\cos\theta_{\rm jet}| < 0.9$) are kept. In addition, there must be two oppositely charged jets. If $M_{12} < 1$ GeV/c^2, then the vector momentum sum of tracks 1 and 2 must make an angle of at least 10° with respect to each charged jet, tightened to 20° if track 1 or 2 is an identified electron. In order to further reject ditau events, the angle between the two charged jets must be less than 170°.

The additional selection for the $\ell^+\ell^-\tau^+\tau^-$ topology increases the signal acceptance for $e^+e^-\tau^+\tau^-$ and $\mu^+\mu^-\tau^+\tau^-$ by more than a factor of two.

Expectations for the four-lepton channel are summarized in Table 2. The total signal expected from the four-lepton channel is 1.59 ± 0.06 events, to be compared to a total expectation of $0.01^{+0.08}_{-0.01}$ events from background. The main background contributions are from $\ell^+\ell^-\gamma$ events. The expectation from the final state with four taus is negligible. The efficiency presented in Table 2 is computed inside the acceptance region defined by FERMISV. Since this analysis has only a two lepton requirement in the $\ell^+\ell^-\ell^+\ell^-$ channel, it can in principle select low-multiplicity $\ell^+\ell^-q\bar{q}$ events with a high mass lepton pair. In addition, when the taus decay hadronically, the $\ell^+\ell^-\tau^+\tau^-$ final state can be indistinguishable from a $\ell^+\ell^-q\bar{q}$ final state. Thus, through both the $\ell^+\ell^-\ell^+\ell^-$ and $\ell^+\ell^-\tau^+\tau^-$ selections, this analysis has a total expectation of 0.32 ± 0.06 events from the $\ell^+\ell^-q\bar{q}$ final state, with a negligible overlap with the selection of the previous section. This corresponds to an increase of $\sim 10\%$ in the signal expectation for $\ell^+\ell^-q\bar{q}$. The assignment of systematic errors is discussed in Section 4.5.

4.4 The neutrino channel

The neutrino channel can be divided into two classes: a "low-multiplicity topology" (two good tracks) and a "higher-multiplicity topology" (four or more good tracks). Both of these classes have very distinct background contributions. The main four-fermion contributions to the low-multiplicity topology come from the $\nu\bar{\nu}e^+e^-$, $\nu\bar{\nu}\mu^+\mu^-$, and $\nu\bar{\nu}u\bar{u}$ final states while the background contributions come mostly from low multiplicity gamma-gamma events and from $\nu\nu\gamma$ events. The higher-multiplicity topology is dominated by the $\nu\bar{\nu}u\bar{u}$ and $\nu\bar{\nu}c\bar{c}$ four-fermion final states with the largest background contribution coming from high-multiplicity gamma-gamma events.

The selections for both topologies use many of the same quantities. The event acoplanarity is formed by dividing the event into two hemispheres along the thrust axis and calculating the angle between the total momentum of each hemisphere projected into a plane perpendicular to the beam axis. In order to reject gamma-gamma and $q\bar{q}$ backgrounds the acoplanarity is required to be less than 130°. Events from gamma-gamma interactions are further rejected by requiring the missing transverse momentum to be greater than $6\%\sqrt{s}$ and that the missing mass, $M_{\rm miss}$, be less than $90\%\sqrt{s}$. One last cut is applied in order to reject gamma-gamma events. The direction of a hypothetical scattered beam electron is calculated assuming the kinematics of gamma-gamma interactions. Events are rejected if there is an energy flow object within 26° of this direction in the low-multiplicity case and 5° of this direction in the higher-multiplicity case.

The low-multiplicity selection is enhanced with some additional requirements. The Bhabha background is eliminated by requiring that each track have a transverse momentum with respect to the beam axis of at least 2 GeV/c and that no single energy flow object have an energy larger than $30\%\sqrt{s}$. High multiplicity events from $\tau\tau$ and $\gamma\gamma \to \tau^+\tau^-$ processes with only two good tracks are rejected by requiring no bad tracks with at least four TPC hits in the event. Background events from $\nu\nu\gamma$ in which the photon converts are eliminated by rejecting events that have an identified converted photon and by requiring that at least one of the good tracks in the event has a VDET hit. It is also required that the sum of the energies of all energy flow objects more than 10° from both tracks does not exceed 5 GeV.

The higher-multiplicity selection also has some additional requirements. Background from $q\bar{q}$ is eliminated by requiring that $M_{\rm miss}$ be greater than $60\%\sqrt{s}$. This background is also rejected by requiring that the energy measured in an azimuthal wedge of half-angle 26° about the direction of missing transverse momentum be less than 3 GeV. Finally, high multiplicity gamma-gamma backgrounds are further rejected by requiring $E_{\rm LCAL} + E_{\rm SICAL}$ to be less than 5 GeV and that at least two charged particle tracks have a transverse momentum with respect to the beam axis of at least 1 GeV/c.

The expectations for the $\nu\bar{\nu}f\bar{f}$ channel are summarized in Table 3. The expected background for the low-multiplicity topology is $0.03 \pm^{0.08}_{0.02}$ events while the signal expectation is 1.74 ± 0.05 events. The expected background for the higher-multiplicity topology is $0.03 \pm^{0.02}_{0.01}$ events while the signal expectation is 0.52 ± 0.02 events.

4.5 Systematic studies

4.5.1 Studies of background and efficiency

The more discriminating measured quantities have been studied in order to validate the background and efficiency estimation.

Since the lepton isolation plays such a crucial role in reducing the $q\bar{q}$ background in the $\ell^+\ell^-q\bar{q}$ channel, checks were performed comparing the isolation in data and Monte Carlo. The

Table 3: Summary of $\nu\bar{\nu}f\bar{f}$ expectations. The uncertainties are statistical only.

Process	$q\bar{q}$	$\ell^+\ell^-\gamma$	$\gamma\gamma \to f\bar{f}$	$\nu\nu\gamma$	$\nu\bar{\nu}\ell^+\ell^-$
N expected (low-mult)	negligible	< 0.01	< 0.07	$0.03 \pm {}^{0.02}_{0.01}$	1.46 ± 0.05
Efficiency		< 0.01	$0.03 \pm {}^{0.02}_{0.01}$	$0.03 \pm {}^{0.04}_{0.02}$	$(41 \pm 1)\%$
N expected (higher-mult)				negligible	–
Efficiency					

Process	$\nu\bar{\nu}\tau^+\tau^-$	$\nu\bar{\nu}q\bar{q}$
N expected (low-mult)	0.01 ± 0.00	0.27 ± 0.02
Efficiency	$(7 \pm 1)\%$	$(11 \pm 1)\%$
N expected (higher-mult)	0.02 ± 0.00	0.50 ± 0.02
Efficiency	$(12 \pm 1)\%$	$(27 \pm 1)\%$

single lepton isolation was studied in hadronic events and good agreement was found between data and Monte Carlo. Fig. 2 shows the distributions of the dilepton isolation $\Theta_{\rm iso}$ for muon and electron pairs, before the isolation cut, and normalized to the integrated luminosity. In order to perform a statistically significant test of the agreement in $\Theta_{\rm iso}$, the lepton requirements were removed and the yield of particle track pairs was compared between the simulation and the data in the region $\Theta_{\rm iso} > 60^\circ$. In this region, the simulation underestimates the data yields by 30%. The background estimates from $q\bar{q}$ have thus been increased by a factor of 1.4. Since only a small fraction of $q\bar{q}$ events are affected by this correction and since most signal events fall in the region $\Theta_{\rm iso} > 60^\circ$ (see Fig. 2), this effect can be neglected in the signal efficiency.

The estimation of the $\nu\nu\gamma$ and Bhabha backgrounds is very sensitive to how well photon conversions are reproduced in the Monte Carlo. The rate of pair conversions in the data was found to agree well with the Monte Carlo predictions. The agreement between the simulation and data is also good within statistical errors (12%) for photons which convert within the VDET volume. Bhabha events pose a dangerous background for the four-lepton channel because their production cross section is large, and because they contain many radiated photons which, when converted, give four-electron events. An inclusive sample of Bhabha events was selected using most of the cuts from the $\ell^+\ell^-\ell^+\ell^-$ topology and the relevant quantities used in the selection were compared in data and Monte Carlo. The limited statistical precision of the comparison of the number of four-track events and the number of converted photons leads to a systematic uncertainty of 18%. The error on this background has been increased by a factor of 1.18. Other backgrounds producing converted photons have been increased in the same way by a factor of 1.12.

The requirement that particle tracks have hits in the VDET has also been used in this analysis to reject conversion electrons. The fraction of particle tracks having no VDET hits was studied and good agreement was found between the data and the simulation. The number of bad tracks, used in the $\ell^+\ell^-\ell^+\ell^-$ and the $\nu\bar{\nu}f\bar{f}$ channels, was studied by comparing Bhabha, $q\bar{q}$, and gamma-gamma events in both data and Monte Carlo simulation. Good agreement was found between data and simulation in the number of bad tracks with at least four TPC hits (relevant to the $\nu\bar{\nu}f\bar{f}$ channel). A 3% systematic error has been assigned to the efficiency and background determination in the $\ell^+\ell^-\ell^+\ell^-$ channel due to the imperfect simulation of the number of bad tracks.

Based on studies of lepton identification at LEP 1 [7], a 3% systematic error has been assigned to the efficiency and background determination of those channels where lepton identification is used.

4.5.2 Uncertainties in signal prediction

The FERMISV program has been modified [1] to include QCD corrections to the production rates. The corrections include the production of resonant states from the photon propagator and quark mass threshold effects in the continuum. Based on the considerations in Ref. [1], a systematic uncertainty of 4% due to these corrections is assigned to the four-fermion final state predictions with hadrons. A systematic uncertainty of 1.1% is assigned to all final states which reflects the missing higher-order QED corrections and the uncertainties in $\sin^2\theta_{\rm W}^{\rm eff}$. In addition, an overall systematic uncertainty of 4% is assigned to all channels in order to account for the difference between the cross section predictions of FERMISV and the predictions of the EXCALIBUR [16] four-fermion Monte Carlo program.

Gluon radiation from high-mass quark pairs reduces the contributions of the annihilation diagrams (Fig. 1b). A correction factor of 0.992 ± 0.008 $[0.985 \pm 0.015]$ is thus applied to the

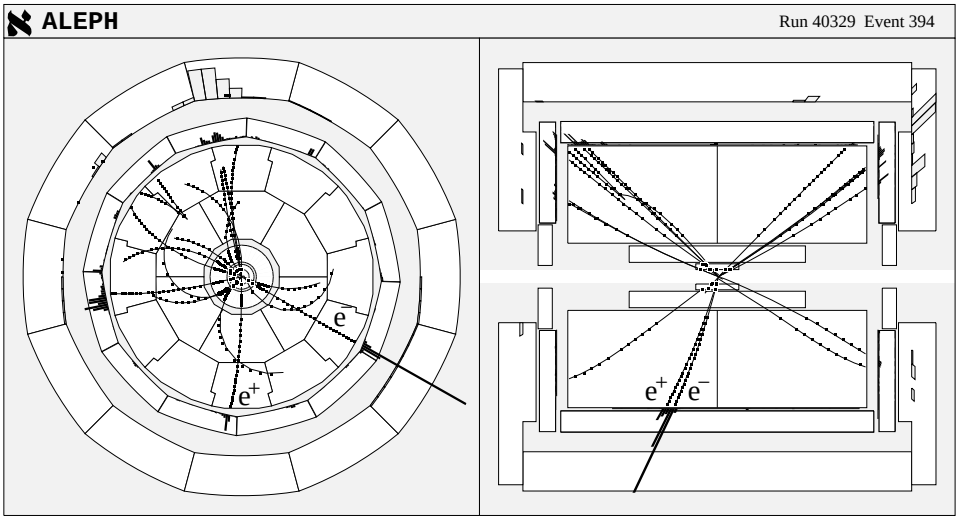

Figure 3: Candidate four-fermion $e^+e^-q\bar{q}$ event. In this event display, the central region has been expanded to emphasize the tracking detectors.

predictions in the $e^+e^-q\bar{q}$ [$\mu^+\mu^-q\bar{q}$] channel. The correction factors were determined, using the arguments of Ref. [1], from the relative contributions of the annihilation diagrams involving quarks at $\sqrt{s}$ = 130 and 136 GeV.

Finally, a 1% systematic uncertainty is assigned to the signal and background predictions due to the luminosity measurement.

5 Results

After analyzing the 5.8 pb^{-1} of data taken during the 1995 high energy run, five events were selected; one event in the $\ell^+\ell^-q\bar{q}$ channel, one event in the $\ell^+\ell^-\ell^+\ell^-$ channel, and three events in the $\nu\bar{\nu}f\bar{f}$ channel.

The selected $\ell^+\ell^-q\bar{q}$ event, shown in Fig. 3, has a well isolated ($\Theta_{iso} = 155^\circ$) electron pair with an invariant mass of 10.7 GeV/c^2. The event has a high multiplicity hadronic system ($N_{ch} = 15$) with a visible mass of 87 GeV/c^2. The mass recoiling against the electron pair, computed using the momenta of the electrons, is 90 GeV/c^2.

The four-lepton candidate event contains four charged particle tracks, three of which are identified as electrons. The fourth electron candidate enters a crack between ECAL modules. The two energetic electrons have momenta of 57 and 25 GeV/c, and their invariant mass is 67 GeV/c^2, lower than expected, but consistent with the four-fermion hypothesis. The low-mass pair consists of two electrons of momenta of 25 and 5.4 GeV/c. Its mass is only 54 MeV/c^2, but each electron has a VDET hit, and the radius of closest approach to the primary vertex is 1.2 cm – far inside the beampipe.

Two of the three $\nu\bar{\nu}f\bar{f}$ candidates passed the low-multiplicity selection. Both tracks in each event are identified as electrons. One event has a dilepton mass of 3.7 GeV/c^2 and a missing mass of 87 GeV/c^2 and the other event has a dilepton mass of 3.5 GeV/c^2 and a missing mass of 115 GeV/c^2. These quantities, and other relevant ones (such as missing transverse momentum), are consistent with the expectations for the signal processes. For the higher-multiplicity event (Fig. 4), none of the tracks are leptons. Thus, both low-multiplicity events are $\nu\bar{\nu}e^+e^-$ candidates while the higher-multiplicity event is a $\nu\bar{\nu}q\bar{q}$ candidate.

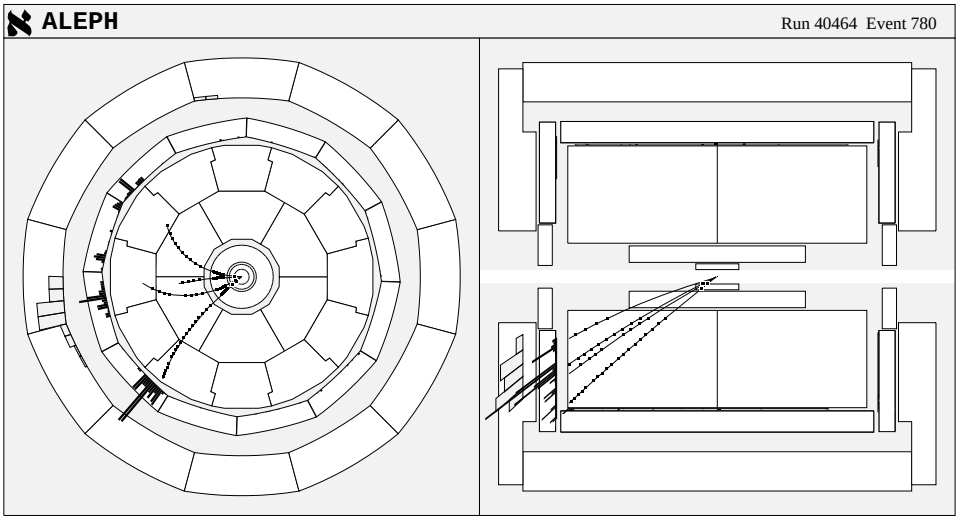

Figure 4: Candidate four-fermion $\nu\bar{\nu}q\bar{q}$ event. In this event display, the central region has been expanded to emphasize the tracking detectors.

The expectations for the three four-fermion topologies considered in this letter, and their backgrounds, are summarized in Table 4. The expectation presented for the $\ell^+\ell^-q\bar{q}$ [$\ell^+\ell^-\ell^+\ell^-$] channel includes the cross-efficiency contribution from the $\ell^+\ell^-\ell^+\ell^-$ [$\ell^+\ell^-q\bar{q}$] channel.

The OPAL collaboration, in an analysis of their 1995 high energy run data, has reported [17] the observation of an excess of events in topologies typical of high-multiplicity four-fermion processes. The results of the study of such processes in the ALEPH data show no excess when compared with the Standard Model predictions.

6 Conclusion

The ALEPH data taken during the 1995 high energy run were examined in order to study the production of $\ell^+\ell^-q\bar{q}$, $\nu\bar{\nu}f\bar{f}$, and $\ell^+\ell^-\ell^+\ell^-$ four-fermion final states. The analyses achieved a low background while retaining a good efficiency for both the low- and high-multiplicity four-fermion processes. Five events were selected in the data, in agreement with the Standard Model expectation of 6.67 ± 0.38 from four-fermion processes and $0.14 \pm^{0.19}_{0.05}$ from background processes.

Acknowledgements

We are indebted to our colleagues in the accelerator divisions for the excellent performance of the LEP storage ring and the impressive startup of the high energy run. We also thank the engineers and technicians of the collaborating institutions for their support in constructing the ALEPH experiment. Those of us from non-member states thank CERN for its hospitality.

References

[1] ALEPH Coll., D. Buskulic et al., Z. Phys. **C 66** (1995) 3.

Table 4: Summary of results for the four-fermion processes. The uncertainties are statistical and systematic, respectively. The statistical and systematic uncertainties have been combined in quadrature in the background expectations.

Process	$\ell^+\ell^-\mathrm{q\bar{q}}$	$\ell^+\ell^-\ell^+\ell^-$	$\nu\bar{\nu}\mathrm{f\bar{f}}$	TOTAL
N expected signal	$2.78 \pm 0.07 \pm 0.18$	$1.63 \pm 0.06 \pm 0.10$	$2.26 \pm 0.05 \pm 0.11$	$6.67 \pm 0.11 \pm 0.37$
N expected background	$0.07 \pm^{0.15}_{0.04}$	$0.01 \pm^{0.08}_{0.01}$	$0.05 \pm^{0.08}_{0.02}$	$0.14 \pm^{0.19}_{0.05}$
N expected total	$2.86 \pm^{0.17}_{0.08} \pm 0.19$	$1.64 \pm^{0.10}_{0.06} \pm 0.10$	$2.31 \pm^{0.10}_{0.06} \pm 0.11$	$6.81 \pm^{0.22}_{0.12} \pm 0.37$
N observed	1	1	3	5

[2] OPAL Coll., P.D. Acton et al., Phys. Lett. **B 287** (1992) 389;
DELPHI Coll., P. Abreu et al., Nucl. Phys. **B 403** (1993) 3;
L3 Coll., A. Adam et al., Phys. Lett. **B 321** (1994) 283.

[3] CELLO Coll., H.-J. Behrend et al., Z. Phys. **C43** (1989) 1;
AMY Coll., Y.H. Ho et al., Phys. Lett. **B 244** (1990) 573;
MARK II Coll., M. Petradza et al., Phys. Rev. **D 42** (1990) 2171;
MARK II Coll., T. Barklow et al., Phys. Rev. Lett. **68** (1992) 13.

[4] ALEPH Coll., D. Buskulic et al., *"Four-jet final state production in* e^+e^- *collisions at centre-of-mass energies of 130 and 136 GeV"*, CERN/PPE 96-52, (April,1996). To be published in Z. Phys C.

[5] ALEPH Coll., D. Decamp et al., Nucl. Instrum. Methods **A 294** (1990) 121.

[6] ALEPH Coll., D. Buskulic et al., Nucl. Instrum. Methods **A 360** (1995) 481.

[7] ALEPH Coll., D. Buskulic et al., Nucl. Instrum. Methods **A 346** (1994) 461.

[8] J.M. Hilgart, R. Kleiss, F. LeDiberder, Comput. Phys. Commun. **75** (1993) 191.

[9] T. Sjöstrand, Comp. Phys. Commun. **82** (1994) 74;
T. Sjöstrand, CERN-TH 7112/93 (1993, revised August 1994).

[10] S. Jadach, Z. Was, Comput. Phys. Commun. **36** (1985) 191.

[11] M. Böhm, A. Denner, W. Hollik, Nucl. Phys. **B 304** (1988) 687;
F.A. Berends, R. Kleiss, W. Hollik, Nucl. Phys. **B 304** (1988) 712.

[12] H. Anlauf et al., Comput. Phys. Commun. **79** (1994) 466.

[13] ALEPH Coll., D. Buskulic et al., Phys. Lett. **B 313** (1993) 509.

[14] M. Drees, R. Godbole, Nucl. Phys. **B 339** (1990) 355.

[15] JADE Coll., W. Bartel et al., Z. Phys **C33** (1986) 23;
JADE Coll., S. Bethke et al., Phys. Lett. **B 213** (1988) 235.

[16] F.A. Berends, R. Pittau, R. Kleiss, Comput. Phys. Comm **85** (1995) 437;
F.A. Berends, R. Pittau, R. Kleiss, Nucl. Phys. **B 424** (1994) 308.

[17] OPAL Coll., G. Alexander et al., *"A study of four-fermion final states with high multiplicity at LEP"*, CERN/PPE 96-31, (March,1996). To be published in Phys. Lett. B.